How can the Odderon be detected at RHIC and LHC

Basarab Nicolescu

Theory Group, LPNHE, CNRS and University Paris 6

Summary

Summary

Summary

Summary

Introduction

- The Odderon is defined as a singularity in the complex J-plane, located at $J = 1$ when $t = 0$ and which contributes to the odd-under-crossing amplitude F_{-}. The concept of Odderon first emerged in 1973 in the context of asymptotic theorems

  L. Lukaszuk and B. Nicolescu, Nuovo Cim. Lett. **8**, 405 (1973)

- The Odderon remains an elusive object, 34 years after its invention.

Introduction

- The Odderon is defined as a singularity in the complex J-plane, located at $J = 1$ when $t = 0$ and which contributes to the odd-under-crossing amplitude F_-. The concept of Odderon first emerged in 1973 in the context of asymptotic theorems

  L. Lukaszuk and B. Nicolescu, Nuovo Cim. Lett. **8**, 405 (1973)

- The Odderon remains an elusive object, 34 years after its invention.

Introduction

In fact, the situation of the Odderon was already nicely summarized in 1881 by Odilon Redon (Kazunori Itakura, private communication, 2005)

The smiling spider

Introduction

In fact, the situation of the Odderon was already nicely summarized in 1881 by Odilon Redon (Kazunori Itakura, private communication, 2005)

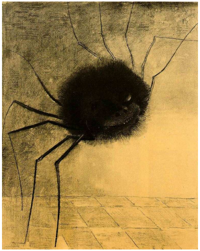

The smiling spider

Introduction

In fact, the situation of the Odderon was already nicely summarized in 1881 by Odilon Redon (Kazunori Itakura, private communication, 2005)

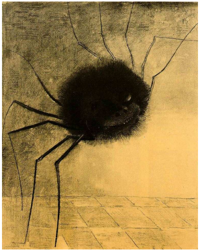

The smiling spider

Introduction

- The Odderon is now a fundamental object in QCD and CGC and it has to be found experimentally if QCD and CGC are right.

- How to find the Odderon at RHIC and LHC?

Regina F. Avila, Pierre Gauron, Basarab Nicolescu,
Eur. Phys. J. **C49**, 581-592 (2007)

Introduction

- The Odderon is now a fundamental object in QCD and CGC and it has to be found experimentally if QCD and CGC are right.

- How to find the Odderon at RHIC and LHC?

  Regina F. Avila, Pierre Gauron, Basarab Nicolescu,

  Eur. Phys. J. **C49**, 581-592 (2007)

The Maximal Odderon

- Special case: maximal asymptotic ($s \to \infty$) behavior allowed by the general principles of strong interactions:

$$\sigma_T(s) \propto \ln^2 s, \quad \text{as } s \to \infty$$

and

$$\Delta\sigma(s) \equiv \sigma_T^{\bar{p}p}(s) - \sigma_T^{pp}(s) \propto \ln s, \quad \text{as } s \to \infty\ .$$

- $\sigma_T(s) \propto \ln^2 s$ first discovered by Heisenberg in 1952

W. Heisenberg, Z. Phys. **133**, 65 (1952)

  - Also proved in the context of the AdS/CFT dual string-gravity theory and of the Color Glass Condensate approach
  - Also shown to provide the best description of the present experimental data on total cross-sections (COMPETE Collaboration)
  - The maximal behavior of $ImF_+(s,t=0) \propto s\ln^2 s$ is naturally associated with the maximal behavior $ImF_-(s,t=0) \propto \ln s$: strong interactions should be as strong as possible

The Maximal Odderon

- Special case: maximal asymptotic ($s \to \infty$) behavior allowed by the general principles of strong interactions:

$$\sigma_T(s) \propto \ln^2 s, \quad \text{as } s \to \infty$$

and

$$\Delta\sigma(s) \equiv \sigma_T^{\bar{p}p}(s) - \sigma_T^{pp}(s) \propto \ln s, \quad \text{as } s \to \infty \,.$$

- $\sigma_T(s) \propto \ln^2 s$ first discovered by Heisenberg in 1952

W. Heisenberg, Z. Phys. **133**, 65 (1952)

- Also proved in the context of the AdS/CFT dual string-gravity theory and of the Color Glass Condensate approach
- Also shown to provide the best description of the present experimental data on total cross-sections (COMPETE Collaboration)
- The maximal behavior of $ImF_+(s, t=0) \propto s \ln^2 s$ is naturally associated with the maximal behavior $ImF_-(s, t=0) \propto \ln s$: strong interactions should be as strong as possible

The Maximal Odderon

- Special case: maximal asymptotic ($s \to \infty$) behavior allowed by the general principles of strong interactions:

$$\sigma_T(s) \propto \ln^2 s, \quad \text{as } s \to \infty$$

and

$$\Delta\sigma(s) \equiv \sigma_T^{\bar{p}p}(s) - \sigma_T^{pp}(s) \propto \ln s, \quad \text{as } s \to \infty \, .$$

- $\sigma_T(s) \propto \ln^2 s$ first discovered by Heisenberg in 1952

W. Heisenberg, Z. Phys. **133**, 65 (1952)

  - Also proved in the context of the AdS/CFT dual string-gravity theory and of the Color Glass Condensate approach
  - Also shown to provide the best description of the present experimental data on total cross-sections (COMPETE Collaboration)
  - The maximal behavior of $ImF_+(s, t = 0) \propto s \ln^2 s$ is naturally associated with the maximal behavior $ImF_-(s, t = 0) \propto \ln s$: strong interactions should be as strong as possible

The Maximal Odderon

- Special case: maximal asymptotic ($s \to \infty$) behavior allowed by the general principles of strong interactions:

$$\sigma_T(s) \propto \ln^2 s, \quad \text{as } s \to \infty$$

and

$$\Delta\sigma(s) \equiv \sigma_T^{\bar{p}p}(s) - \sigma_T^{pp}(s) \propto \ln s, \quad \text{as } s \to \infty \, .$$

- $\sigma_T(s) \propto \ln^2 s$ first discovered by Heisenberg in 1952

W. Heisenberg, Z. Phys. **133**, 65 (1952)

  - Also proved in the context of the AdS/CFT dual string-gravity theory and of the Color Glass Condensate approach
  - Also shown to provide the best description of the present experimental data on total cross-sections (COMPETE Collaboration)
  - The maximal behavior of $ImF_+(s, t = 0) \propto s \ln^2 s$ is naturally associated with the maximal behavior $ImF_-(s, t = 0) \propto \ln s$: strong interactions should be as strong as possible

The Maximal Odderon

- Special case: maximal asymptotic ($s \to \infty$) behavior allowed by the general principles of strong interactions:

$$\sigma_T(s) \propto \ln^2 s, \quad \text{as } s \to \infty$$

and

$$\Delta\sigma(s) \equiv \sigma_T^{\bar{p}p}(s) - \sigma_T^{pp}(s) \propto \ln s, \quad \text{as } s \to \infty \, .$$

- $\sigma_T(s) \propto \ln^2 s$ first discovered by Heisenberg in 1952

W. Heisenberg, Z. Phys. **133**, 65 (1952)

  - Also proved in the context of the AdS/CFT dual string-gravity theory and of the Color Glass Condensate approach
  - Also shown to provide the best description of the present experimental data on total cross-sections (COMPETE Collaboration)
  - The maximal behavior of $ImF_+(s, t = 0) \propto s \ln^2 s$ is naturally associated with the maximal behavior $ImF_-(s, t = 0) \propto \ln s$: strong interactions should be as strong as possible

Strategy

- We consider two cases: one in which the Odderon is absent and one in which the Odderon is present.
- We use the two respective forms in order to describe the 832 experimental points for pp and $\bar{p}p$ scattering, from PDG Tables, for $\sigma_T(s)$, $\rho(s)$ and $d\sigma/dt(s,t)$, in the s-range

$$4.539 \text{ GeV} \leqslant \sqrt{s} \leqslant 1800 \text{ GeV}$$

and in the t-range

$$0 \leqslant |t| \leqslant 2.6 \text{ GeV}^2 .$$

The best form will be chosen.
- In order to make predictions at RHIC and LHC energies, we will insist on the best possible *quantitative* description of the data. Most of the existing phenomenological models describe only the gross features of the data in a limited region of energy and therefore they could lead to wrong quantitative predictions at much higher energies.
- From the study of the interference between $F_+(s,t)$ and $F_-(s,t)$ amplitudes we will conclude which are the best experiments to be done in order to detect in a clear way the Odderon.

Strategy

- We consider two cases: one in which the Odderon is absent and one in which the Odderon is present.
- We use the two respective forms in order to describe the 832 experimental points for pp and $\bar{p}p$ scattering, from PDG Tables, for $\sigma_T(s)$, $\rho(s)$ and $d\sigma/dt(s,t)$, in the s-range

$$4.539 \text{ GeV } \leqslant \sqrt{s} \leqslant 1800 \text{ GeV}$$

and in the t-range

$$0 \leqslant |t| \leqslant 2.6 \text{ GeV}^2 .$$

The best form will be chosen.

- In order to make predictions at RHIC and LHC energies, we will insist on the best possible *quantitative* description of the data. Most of the existing phenomenological models describe only the gross features of the data in a limited region of energy and therefore they could lead to wrong quantitative predictions at much higher energies.
- From the study of the interference between $F_+(s,t)$ and $F_-(s,t)$ amplitudes we will conclude which are the best experiments to be done in order to detect in a clear way the Odderon.

Strategy

- We consider two cases: one in which the Odderon is absent and one in which the Odderon is present.
- We use the two respective forms in order to describe the 832 experimental points for pp and $\bar{p}p$ scattering, from PDG Tables, for $\sigma_T(s)$, $\rho(s)$ and $d\sigma/dt(s,t)$, in the s-range

$$4.539 \text{ GeV } \leqslant \sqrt{s} \leqslant 1800 \text{ GeV}$$

  and in the t-range

$$0 \leqslant |t| \leqslant 2.6 \text{ GeV}^2 \ .$$

  The best form will be chosen.
- In order to make predictions at RHIC and LHC energies, we will insist on the best possible *quantitative* description of the data. Most of the existing phenomenological models describe only the gross features of the data in a limited region of energy and therefore they could lead to wrong quantitative predictions at much higher energies.
- From the study of the interference between $F_+(s,t)$ and $F_-(s,t)$ amplitudes we will conclude which are the best experiments to be done in order to detect in a clear way the Odderon.

Strategy

- We consider two cases: one in which the Odderon is absent and one in which the Odderon is present.
- We use the two respective forms in order to describe the 832 experimental points for *pp* and $\bar{p}p$ scattering, from PDG Tables, for $\sigma_T(s)$, $\rho(s)$ and $d\sigma/dt(s,t)$, in the s-range

  $$4.539 \text{ GeV } \leqslant \sqrt{s} \leqslant 1800 \text{ GeV}$$

  and in the t-range

  $$0 \leqslant |t| \leqslant 2.6 \text{ GeV}^2 \ .$$

  The best form will be chosen.
- In order to make predictions at RHIC and LHC energies, we will insist on the best possible *quantitative* description of the data. Most of the existing phenomenological models describe only the gross features of the data in a limited region of energy and therefore they could lead to wrong quantitative predictions at much higher energies.
- From the study of the interference between $F_+(s,t)$ and $F_-(s,t)$ amplitudes we will conclude which are the best experiments to be done in order to detect in a clear way the Odderon.

Definition of the amplitudes

- $F_{\pm}(s,t) = \frac{1}{2}\left(F_{pp}(s,t) \pm F_{\bar{p}p}(s,t)\right), F_{\pm} \sim$ even(odd)-under-crossing
- $F_{+}(s,t) = F_{+}^{H}(s,t) + F_{+}^{P}(s,t) + F_{+}^{PP}(s,t) + F_{+}^{R}(s,t) + F_{+}^{RP}(s,t)$.
  $F_{-}(s,t) = F_{-}^{MO}(s,t) + F_{-}^{O}(s,t) + F_{-}^{OP}(s,t) + F_{-}^{R}(s,t) + F_{-}^{RP}(s,t)$.
- $F_{pp}(s,t) = F_{+}(s,t) + F_{-}(s,t)$
  $F_{\bar{p}p}(s,t) = F_{+}(s,t) - F_{-}(s,t)$
- Normalization

$$\sigma_T(s) = \frac{1}{s}\mathrm{Im}F(s,0)\,, \quad \rho(s) = \frac{\mathrm{Re}F(s,t=0)}{\mathrm{Im}F(s,t=0)}$$

$$\frac{d\sigma}{dt}(s,t) = \frac{1}{16\pi s^2}|F(s,t)|^2\,.$$

Definition of the amplitudes

- $F_{\pm}(s,t) = \frac{1}{2}\left(F_{pp}(s,t) \pm F_{\bar{p}p}(s,t)\right), F_{\pm} \sim$ even(odd)-under-crossing
- $F_{+}(s,t) = F_{+}^{H}(s,t) + F_{+}^{P}(s,t) + F_{+}^{PP}(s,t) + F_{+}^{R}(s,t) + F_{+}^{RP}(s,t)$.
  $F_{-}(s,t) = F_{-}^{MO}(s,t) + F_{-}^{O}(s,t) + F_{-}^{OP}(s,t) + F_{-}^{R}(s,t) + F_{-}^{RP}(s,t)$.
- $F_{pp}(s,t) = F_{+}(s,t) + F_{-}(s,t)$
  $F_{\bar{p}p}(s,t) = F_{+}(s,t) - F_{-}(s,t)$
- Normalization

$$\sigma_T(s) = \frac{1}{s}\mathrm{Im}F(s,0)\,, \quad \rho(s) = \frac{\mathrm{Re}F(s,t=0)}{\mathrm{Im}F(s,t=0)}$$

$$\frac{d\sigma}{dt}(s,t) = \frac{1}{16\pi s^2}|F(s,t)|^2\,.$$

Definition of the amplitudes

- $F_\pm(s,t) = \frac{1}{2}\left(F_{pp}(s,t) \pm F_{\bar{p}p}(s,t)\right), F_\pm \sim$ even(odd)-under-crossing

- $F_+(s,t) = F_+^H(s,t) + F_+^P(s,t) + F_+^{PP}(s,t) + F_+^R(s,t) + F_+^{RP}(s,t)$.
  $F_-(s,t) = F_-^{MO}(s,t) + F_-^O(s,t) + F_-^{OP}(s,t) + F_-^R(s,t) + F_-^{RP}(s,t)$.

- $F_{pp}(s,t) = F_+(s,t) + F_-(s,t)$
  $F_{\bar{p}p}(s,t) = F_+(s,t) - F_-(s,t)$

- Normalization

$$\sigma_T(s) = \frac{1}{s}\mathrm{Im}F(s,0)\,, \quad \rho(s) = \frac{\mathrm{Re}F(s,t=0)}{\mathrm{Im}F(s,t=0)}$$

$$\frac{d\sigma}{dt}(s,t) = \frac{1}{16\pi s^2}|F(s,t)|^2\,.$$

Definition of the amplitudes

- $F_\pm(s,t) = \frac{1}{2}\left(F_{pp}(s,t) \pm F_{\bar{p}p}(s,t)\right), F_\pm \sim$ even(odd)-under-crossing
- $F_+(s,t) = F_+^H(s,t) + F_+^P(s,t) + F_+^{PP}(s,t) + F_+^R(s,t) + F_+^{RP}(s,t)$.
  $F_-(s,t) = F_-^{MO}(s,t) + F_-^O(s,t) + F_-^{OP}(s,t) + F_-^R(s,t) + F_-^{RP}(s,t)$.
- $F_{pp}(s,t) = F_+(s,t) + F_-(s,t)$
  $F_{\bar{p}p}(s,t) = F_+(s,t) - F_-(s,t)$
- Normalization

$$\sigma_T(s) = \frac{1}{s}\mathrm{Im}F(s,0)\,, \quad \rho(s) = \frac{\mathrm{Re}F(s,t=0)}{\mathrm{Im}F(s,t=0)}$$

$$\frac{d\sigma}{dt}(s,t) = \frac{1}{16\pi s^2}|F(s,t)|^2\,.$$

The Heisenberg $F_+^H(s,t)$ amplitude

$$\begin{aligned}\frac{1}{is}F_+^H(s,t) &= H_1 \ln^2 \bar{s}\ \frac{2J_1(K_+\bar{\tau})}{K_+\bar{\tau}} \exp(b_1^+ t) \\ &+ H_2 \ln \bar{s} J_0(K_+\bar{\tau}) \exp(b_2^+ t) \\ &+ H_3[J_0(K_+\bar{\tau}) - K_+\bar{\tau} J_1(K_+\bar{\tau})] \exp(b_3^+ t)\ ,\end{aligned}$$

- Contribution of a 3/2 - cut collapsing, at $t = 0$, to a triple pole located at $J = 1$ and which satisfies the Auberson-Kinoshita-Martin asymptotic theorem

  G. Auberson, T. Kinoshita, and A. Martin, Phys. Rev. **D3**, 3185 (1971)

- $$\begin{aligned}&J_n \to \text{ Bessel functions} \\ &H_k,\ b_k^+ (k = 1,2,3) \text{ and } K_+ \to \text{ constants} \\ &\bar{s} = \left(\frac{s}{s_0}\right) \exp\left(-\frac{1}{2} i\pi\right),\ \text{ with } s_0 = 1 \text{ GeV}^2 \\ &\bar{\tau} = \left(-\frac{t}{t_0}\right)^{1/2} \ln \bar{s}, \quad \text{ with } t_0 = 1 \text{ GeV}^2\ .\end{aligned}$$

The Heisenberg $F_+^H(s,t)$ amplitude

$$\begin{aligned}\frac{1}{is}F_+^H(s,t) &= H_1 \ln^2 \bar{s}\ \frac{2J_1(K_+\bar{\tau})}{K_+\bar{\tau}} \exp(b_1^+ t) \\ &+ H_2 \ln \bar{s} J_0(K_+\bar{\tau}) \exp(b_2^+ t) \\ &+ H_3 [J_0(K_+\bar{\tau}) - K_+\bar{\tau} J_1(K_+\bar{\tau})] \exp(b_3^+ t)\ ,\end{aligned}$$

- Contribution of a 3/2 - cut collapsing, at $t=0$, to a triple pole located at $J=1$ and which satisfies the Auberson-Kinoshita-Martin asymptotic theorem

  G. Auberson, T. Kinoshita, and A. Martin, Phys. Rev. **D3**, 3185 (1971)

- $$\begin{aligned} &J_n \longrightarrow \text{ Bessel functions} \\ &H_k,\ b_k^+ (k=1,2,3) \text{ and } K_+ \longrightarrow \text{constants} \\ &\bar{s} = \left(\frac{s}{s_0}\right) \exp\left(-\tfrac{1}{2} i\pi\right),\ \text{ with } s_0 = 1\ \mathrm{GeV}^2 \\ &\bar{\tau} = \left(-\frac{t}{t_0}\right)^{1/2} \ln \bar{s}, \quad \text{with } t_0 = 1\ \mathrm{GeV}^2\ .\end{aligned}$$

The contribution of the Pomeron Regge pole $F_+^P(s,t)$

$$\frac{1}{s}F_+^P(s,t) = C_P \exp(\beta_P t)[i - \cot(\tfrac{\pi}{2}\alpha_P(t))]\left(\frac{s}{s_0}\right)^{\alpha_P(t)-1} ,$$

- $C_P,\ \beta_P \to$ constants,
- $\alpha_P(t) = \alpha_P(0) + \alpha'_P t$,
- $\alpha_P(0) = 1$,
- $\alpha'_P = 0.25\ \mathrm{GeV}^{-2}$.

The contribution of the Pomeron Regge pole $F_+^P(s,t)$

$$\frac{1}{s}F_+^P(s,t) = C_P \exp(\beta_P t)[i - \cot(\tfrac{\pi}{2}\alpha_P(t))] \left(\frac{s}{s_0}\right)^{\alpha_P(t)-1} ,$$

- $C_P,\ \beta_P \to$ constants,
- $\alpha_P(t) = \alpha_P(0) + \alpha'_P t$,
- $\alpha_P(0) = 1$,
- $\alpha'_P = 0.25\ \text{GeV}^{-2}$.

The contribution of the Pomeron-Pomeron Regge cut $F_+^{PP}(s,t)$

$$\frac{1}{s}F_+^{PP}(s,t) = C_{PP}\exp(\beta_{PP}t)[i\sin(\frac{\pi}{2}\alpha_{PP}(t)) - \cos(\frac{\pi}{2}\alpha_{PP}(t))] \times \frac{(s/s_0)^{\alpha_{PP}(t)-1}}{\ln[(s/s_0)\exp(-\frac{1}{2}i\pi)]} ,$$

- C_{PP}, $\beta_{PP} \to$ constants,
- $\alpha_{PP}(t) = \alpha_{PP}(0) + \alpha'_{PP}t$,
- $\alpha_{PP}(0) = 1$,
- $\alpha'_{PP} = \frac{1}{2}\alpha'_P$.

The contribution of the Pomeron-Pomeron Regge cut $F_+^{PP}(s,t)$

$$\frac{1}{s}F_+^{PP}(s,t) = C_{PP}\exp(\beta_{PP}t)[i\sin(\frac{\pi}{2}\alpha_{PP}(t)) - \cos(\frac{\pi}{2}\alpha_{PP}(t))] \times \frac{(s/s_0)^{\alpha_{PP}(t)-1}}{\ln[(s/s_0)\exp(-\frac{1}{2}i\pi)]},$$

- $C_{PP},\ \beta_{PP} \rightarrow$ constants,
- $\alpha_{PP}(t) = \alpha_{PP}(0) + \alpha'_{PP}t$,
- $\alpha_{PP}(0) = 1$,
- $\alpha'_{PP} = \frac{1}{2}\alpha'_P$.

The contribution of a secondary Regge (f_0, a_0) trajectory whose intercept is around $J = 1/2$

$$\frac{1}{s}F_+^R(s,t) = C_R^+ \gamma_R^+(t) \exp(\beta_R^+ t)[i - \cot(\tfrac{1}{2}\pi\alpha_R^+(t))] \left(\frac{s}{s_0}\right)^{\alpha_R^+(t)-1} ,$$

- $\alpha_R^+(t) = \alpha_R^+(0) + (\alpha_R')^+ t$,
- $(\alpha_R')^+ = 0.88\ GeV^{-2}$ (world phenomenological value)
- $\gamma_R^+(t) = \dfrac{\alpha_R^+(t)[\alpha_R^+(t)+1][\alpha_R^+(t)+2]}{\alpha_R^+(0)[\alpha_R^+(0)+1][\alpha_R^+(0)+2]}$,
- $C_R^+,\ \beta_R^+,\ \alpha_R^+(0) \rightarrow$ constants

The contribution of a secondary Regge (f_0, a_0) trajectory whose intercept is around $J = 1/2$

$$\frac{1}{s} F_+^R(s,t) = C_R^+ \gamma_R^+(t) \exp(\beta_R^+ t)[i - \cot(\tfrac{1}{2}\pi\alpha_R^+(t))] \left(\frac{s}{s_0}\right)^{\alpha_R^+(t)-1} ,$$

- $\alpha_R^+(t) = \alpha_R^+(0) + (\alpha_R')^+ t$,
- $(\alpha_R')^+ = 0.88\ GeV^{-2}$ (world phenomenological value)
- $\gamma_R^+(t) = \dfrac{\alpha_R^+(t)[\alpha_R^+(t)+1][\alpha_R^+(t)+2]}{\alpha_R^+(0)[\alpha_R^+(0)+1][\alpha_R^+(0)+2]}$,
- $C_R^+,\ \beta_R^+,\ \alpha_R^+(0) \rightarrow$ constants

The contribution of the reggeon-Pomeron Regge cut $F_+^{RP}(s,t)$

$$\frac{1}{s}F_+^{RP}(s,t) = \left(\frac{t}{t_0}\right)^2 C_{RP}^+ \exp(\beta_{RP}^+ t)[i\sin(\frac{\pi}{2}\alpha_{RP}^+(t)) - \cos(\frac{\pi}{2}\alpha_{RP}^+(t))] \times \frac{(s/s_0)^{\alpha_{RP}^+(t)-1}}{\ln[(s/s_0)\exp(-\frac{1}{2}i\pi)]},$$

- $\alpha_{RP}^+(t) = \alpha_{RP}^+(0) + (\alpha'_{RP})^+ t$,
- $(\alpha'_{RP})^+ = \frac{(\alpha'_R)^+\alpha'_P}{(\alpha'_R)^+ + \alpha'_P}$
- $C_{RP}^+,\ \beta_{RP}^+,\ \alpha_{RP}^+(0) \to$ constants

The contribution of the reggeon-Pomeron Regge cut $F_+^{RP}(s,t)$

$$\frac{1}{s}F_+^{RP}(s,t) = \left(\frac{t}{t_0}\right)^2 C_{RP}^+ \exp(\beta_{RP}^+ t)[i\sin(\frac{\pi}{2}\alpha_{RP}^+(t)) - \cos(\frac{\pi}{2}\alpha_{RP}^+(t))] \times \frac{(s/s_0)^{\alpha_{RP}^+(t)-1}}{\ln[(s/s_0)\exp(-\frac{1}{2}i\pi)]},$$

- $\alpha_{RP}^+(t) = \alpha_{RP}^+(0) + (\alpha'_{RP})^+ t$,
- $(\alpha'_{RP})^+ = \frac{(\alpha'_R)^+ \alpha'_P}{(\alpha'_R)^+ + \alpha'_P}$
- $C_{RP}^+,\ \beta_{RP}^+,\ \alpha_{RP}^+(0) \rightarrow$ constants

The contribution of the maximal Odderon $F_{-}^{MO}(s,t)$

$$\frac{1}{s}F_{-}^{MO}(s,t) = O_1 \ln^2 \bar{s}\, \frac{\sin(K_{-}\bar{\tau})}{K_{-}\bar{\tau}} \exp(b_1^{-} t) + O_2 \ln \bar{s} \cos(K_{-}\bar{\tau}) \exp(b_2^{-} t) + O_3 \exp(b_3^{-} t)\ ,$$

- Contribution of two complex conjugate poles collapsing, at $t = 0$, to a dipole located at $J = 1$
- Satisfies the Auberson-Kinoshita-Martin asymptotic theorem
- $O_k,\ b_k^{-} (k = 1, 2, 3),\ K_{-} \to$ constants.

The contribution of the maximal Odderon $F_{-}^{MO}(s,t)$

$$\frac{1}{s}F_{-}^{MO}(s,t) = O_1 \ln^2 \bar{s}\, \frac{\sin(K_{-}\bar{\tau})}{K_{-}\bar{\tau}} \exp(b_1^{-} t) + O_2 \ln \bar{s} \cos(K_{-}\bar{\tau}) \exp(b_2^{-} t) + O_3 \exp(b_3^{-} t)\ ,$$

- Contribution of two complex conjugate poles collapsing, at $t = 0$, to a dipole located at $J = 1$
- Satisfies the Auberson-Kinoshita-Martin asymptotic theorem
- $O_k,\ b_k^{-} (k = 1, 2, 3),\ K_{-} \rightarrow$ constants.

The contribution of the maximal Odderon $F_{-}^{MO}(s,t)$

$$\frac{1}{s}F_{-}^{MO}(s,t) = O_1 \ln^2 \bar{s}\,\frac{\sin(K_-\bar{\tau})}{K_-\bar{\tau}}\exp(b_1^- t) + O_2 \ln \bar{s}\cos(K_-\bar{\tau})\exp(b_2^- t) + O_3 \exp(b_3^- t)\ ,$$

- Contribution of two complex conjugate poles collapsing, at $t = 0$, to a dipole located at $J = 1$
- Satisfies the Auberson-Kinoshita-Martin asymptotic theorem
- $O_k,\ b_k^-(k = 1,2,3),\ K_- \to$ constants.

The contribution of the maximal Odderon $F_{-}^{MO}(s,t)$

$$\frac{1}{s}F_{-}^{MO}(s,t) = O_1 \ln^2 \bar{s}\, \frac{\sin(K_{-}\bar{\tau})}{K_{-}\bar{\tau}} \exp(b_1^{-} t) + O_2 \ln \bar{s} \cos(K_{-}\bar{\tau}) \exp(b_2^{-} t) + O_3 \exp(b_3^{-} t)\ ,$$

- Contribution of two complex conjugate poles collapsing, at $t = 0$, to a dipole located at $J = 1$
- Satisfies the Auberson-Kinoshita-Martin asymptotic theorem
- $O_k,\ b_k^{-} (k = 1, 2, 3),\ K_{-} \rightarrow$ constants.

The contribution of the minimal Odderon Regge pole $F_-^O(s,t)$

$$\frac{1}{s}F_-^O(s,t) = C_O \exp(\beta_O t)[i+\tan(\tfrac{1}{2}\pi\alpha_O(t))]\left(\frac{s}{s_0}\right)^{\alpha_O(t)-1}[1+\alpha_O(t)][1-\alpha_O(t)]\,,$$

- $\alpha_O(t) = \alpha_O(0) + \alpha'_O t$,
- $\alpha_O(0) = 1$,
- $C_O\ \beta_O \rightarrow$ constants.

The contribution of the minimal Odderon Regge pole $F_{-}^{O}(s,t)$

$$\frac{1}{s}F_{-}^{O}(s,t) = C_O \exp(\beta_O t)[i+\tan(\tfrac{1}{2}\pi\alpha_O(t))]\left(\frac{s}{s_0}\right)^{\alpha_O(t)-1}[1+\alpha_O(t)][1-\alpha_O(t)]\,,$$

- $\alpha_O(t) = \alpha_O(0) + \alpha'_O t$,
- $\alpha_O(0) = 1$,
- C_O β_O $\rightarrow$ constants.

The contribution of the minimal Odderon-Pomeron Regge cut F_-^{OP}

$$\frac{1}{s}F_-^{OP}(s,t) = C_{OP}\exp(\beta_{OP}t)[\sin(\frac{1}{2}\pi\alpha_{OP}(t))+i\cos(\frac{1}{2}\pi\alpha_{OP}(t))] \times \frac{(s/s_0)^{\alpha_{OP}(t)-1}}{\ln[(s/s_0)\exp(-\frac{1}{2}i\pi)]},$$

- $\alpha_{OP}(t) = \alpha_{OP}(0) + \alpha'_{OP}t$,
- $\alpha_{OP}(0) = 1$,
- $\alpha'_{OP} = \dfrac{\alpha'_O \cdot \alpha'_P}{\alpha'_O + \alpha'_P}$,
- C_{OP} , $\beta_{OP} \rightarrow$ constants.

The contribution of the minimal Odderon-Pomeron Regge cut F_-^{OP}

$$\frac{1}{s}F_-^{OP}(s,t) = C_{OP}\exp(\beta_{OP}t)[\sin(\frac{1}{2}\pi\alpha_{OP}(t)) + i\cos(\frac{1}{2}\pi\alpha_{OP}(t))] \times \frac{(s/s_0)^{\alpha_{OP}(t)-1}}{\ln[(s/s_0)\exp(-\frac{1}{2}i\pi)]},$$

- $\alpha_{OP}(t) = \alpha_{OP}(0) + \alpha'_{OP}t$,
- $\alpha_{OP}(0) = 1$,
- $\alpha'_{OP} = \dfrac{\alpha'_O \cdot \alpha'_P}{\alpha'_O + \alpha'_P}$,
- C_{OP} , $\beta_{OP} \rightarrow$ constants.

The contribution of a secondary Regge (ρ, ω) trajectory whose intercept is around $J = 1/2$

$$\frac{1}{s} F_{-}^{R}(s,t) = -C_R^{-} \gamma_R^{-}(t) \exp(\beta_R^{-} t)[i + \tan(\frac{1}{2}\pi\alpha_R^{-}(t))] \left(\frac{s}{s_0}\right)^{\alpha_R^{-}(t)-1} ,$$

- $\alpha_R^{-}(t) = \alpha_R^{-}(0) + (\alpha_R')^{-} t$,
- $\alpha_{OP}(0) = 1$,
- $(\alpha_R')^{-} = 0.88\ \mathrm{GeV}^{-2}$,
- $C_R^{-},\ \beta_R^{-},\ \alpha_R^{-}(0) \rightarrow$ constants.

The contribution of a secondary Regge (ρ, ω) trajectory whose intercept is around $J = 1/2$

$$\frac{1}{s} F_{-}^{R}(s,t) = -C_R^{-} \gamma_R^{-}(t) \exp(\beta_R^{-} t)[i + \tan(\frac{1}{2}\pi\alpha_R^{-}(t))] \left(\frac{s}{s_0}\right)^{\alpha_R^{-}(t)-1} ,$$

- $\alpha_R^{-}(t) = \alpha_R^{-}(0) + (\alpha_R')^{-} t$,
- $\alpha_{OP}(0) = 1$,
- $(\alpha_R')^{-} = 0.88 \text{ GeV}^{-2}$,
- $C_R^{-}, \ \beta_R^{-}, \ \alpha_R^{-}(0) \rightarrow$ constants.

The contribution of the Reggeon-Pomeron Regge cut F_-^{RP}

$$\frac{1}{s}F_-^{RP}(s,t) = \left(\frac{t}{t_0}\right)^2 C_{RP}^- \exp(\beta_{RP}^- t)[\sin(\frac{\pi}{2}\alpha_{RP}^-(t)) + i\cos(\frac{\pi}{2}\alpha_{RP}^-(t))] \times \frac{(s/s_0)^{\alpha_{RP}^-(t)-1}}{\ln[(s/s_0)\exp(-\frac{1}{2}i\pi)]},$$

- $\alpha_{RP}^-(t) = \alpha_{RP}^-(0) + (\alpha'_{RP})^- t$,
- $(\alpha'_{RP})^- = \dfrac{(\alpha'_R)^-\alpha'_P}{(\alpha'_R)^- + \alpha'_P}$,
- $(\alpha'_R)^- = 0.88\ \mathrm{GeV}^{-2}$,
- $C_{RP}^-,\ \beta_{RP}^-,\ \alpha_{RP}^-(0) \to$ constants.

The contribution of the Reggeon-Pomeron Regge cut F_{-}^{RP}

$$\frac{1}{s}F_{-}^{RP}(s,t) = \left(\frac{t}{t_0}\right)^2 C_{RP}^{-} \exp(\beta_{RP}^{-} t)[\sin(\frac{\pi}{2}\alpha_{RP}^{-}(t)) + i\cos(\frac{\pi}{2}\alpha_{RP}^{-}(t))] \times \frac{(s/s_0)^{\alpha_{RP}^{-}(t)-1}}{\ln[(s/s_0)\exp(-\frac{1}{2}i\pi)]} ,$$

- $\alpha_{RP}^{-}(t) = \alpha_{RP}^{-}(0) + (\alpha'_{RP})^{-} t$,
- $(\alpha'_{RP})^{-} = \dfrac{(\alpha'_{R})^{-}\alpha'_{P}}{(\alpha'_{R})^{-} + \alpha'_{P}}$,
- $(\alpha'_{R})^{-} = 0.88\ \text{GeV}^{-2}$,
- $C_{RP}^{-},\ \beta_{RP}^{-},\ \alpha_{RP}^{-}(0) \rightarrow$ constants.

The case without the Odderon

- $O_k = 0$ $(k = 1, 2, 3)$, $C_O = 0$, $C_{OP} = 0$
- 23 free parameters: H_k, b_k^+ $(k = 1, 2, 3)$, K_+, C_P, β_P, C_{PP}, β_{PP}, C_R^+, β_R^+, $\alpha_R^+(0)$, C_{RP}^+, β_{RP}^+, $\alpha_{RP}^+(0)$, C_R^-, β_R^-, $\alpha_R^-(0)$, C_{RP}^-, β_{RP}^- and $\alpha_{RP}^-(0)$
- $\chi^2/dof = 14.2$
- the no-Odderon case describes nicely the data in the t-region $0 \leqslant |t| \leqslant 0.6$ GeV^2, but totally fails to describe the data for higher t-values
- need for the Odderon

The case without the Odderon

- $O_k = 0 \; (k = 1, 2, 3), \quad C_O = 0, \quad C_{OP} = 0$
- 23 free parameters:
  $H_k,\ b_k^+ \; (k = 1, 2, 3),\ K_+,\ C_P,\ \beta_P,\ C_{PP},\ \beta_{PP},\ C_R^+,$
  $\beta_R^+,\ \alpha_R^+(0),\ C_{RP}^+,\ \beta_{RP}^+, \alpha_{RP}^+(0),\ C_R^-,\ \beta_R^-,\ \alpha_R^-(0),\ C_{RP}^-,\ \beta_{RP}^-$
  and $\alpha_{RP}^-(0)$
- $\chi^2/dof = 14.2$
- the no-Odderon case describes nicely the data in the t-region $0 \leqslant |t| \leqslant 0.6$ GeV^2, but totally fails to describe the data for higher t-values
- need for the Odderon

The case without the Odderon

- $O_k = 0 \ (k = 1, 2, 3), \quad C_O = 0, \quad C_{OP} = 0$
- 23 free parameters:
  $H_k,\ b_k^+ \ (k = 1, 2, 3),\ K_+,\ C_P,\ \beta_P,\ C_{PP},\ \beta_{PP},\ C_R^+,\ \beta_R^+,\ \alpha_R^+(0),\ C_{RP}^+,\ \beta_{RP}^+, \alpha_{RP}^+(0),\ C_R^-,\ \beta_R^-,\ \alpha_R^-(0),\ C_{RP}^-,\ \beta_{RP}^-$ and $\alpha_{RP}^-(0)$
- $\chi^2/dof = 14.2$
- the no-Odderon case describes nicely the data in the t-region $0 \leqslant |t| \leqslant 0.6$ GeV^2, but totally fails to describe the data for higher t-values
- need for the Odderon

The case without the Odderon

- $O_k = 0 \; (k = 1, 2, 3), \quad C_O = 0, \quad C_{OP} = 0$
- 23 free parameters:
  $H_k,\ b_k^+ \ (k = 1, 2, 3),\ K_+,\ C_P,\ \beta_P,\ C_{PP},\ \beta_{PP},\ C_R^+,$
  $\beta_R^+,\ \alpha_R^+(0),\ C_{RP}^+,\ \beta_{RP}^+, \alpha_{RP}^+(0),\ C_R^-,\ \beta_R^-,\ \alpha_R^-(0),\ C_{RP}^-,\ \beta_{RP}^-$
  and $\alpha_{RP}^-(0)$
- $\chi^2/dof = 14.2$
- the no-Odderon case describes nicely the data in the t-region $0 \leqslant |t| \leqslant 0.6$ GeV^2, but totally fails to describe the data for higher t-values
- need for the Odderon

The case without the Odderon

- $O_k = 0 \ (k = 1, 2, 3), \quad C_O = 0, \quad C_{OP} = 0$
- 23 free parameters:
  $H_k,\ b_k^+ \ (k = 1, 2, 3),\ K_+,\ C_P,\ \beta_P,\ C_{PP},\ \beta_{PP},\ C_R^+,$
  $\beta_R^+,\ \alpha_R^+(0),\ C_{RP}^+,\ \beta_{RP}^+, \alpha_{RP}^+(0),\ C_R^-,\ \beta_R^-,\ \alpha_R^-(0),\ C_{RP}^-,\ \beta_{RP}^-$
  and $\alpha_{RP}^-(0)$
- $\chi^2/dof = 14.2$
- the no-Odderon case describes nicely the data in the t-region $0 \leqslant |t| \leqslant 0.6$ GeV^2, but totally fails to describe the data for higher t-values
- need for the Odderon

The case with the Odderon

- 12 supplementary free parameters as compared with the no-Odderon case: $O_k,\ b_k^-$ $(k = 1, 2, 3),\ K_-,\ C_O,\ \beta_O,\ \alpha'_O,\ C_{OP}$ and β_{OP}
- The 23 free parameters associated with the dominant $F_+(s,t)$ amplitude and with the component of $F_-(s,t)$ responsible for describing the data for $\Delta\sigma(s)$ and $\Delta\rho(s, t = 0)$, where

$$\Delta\rho(s, t = 0) \equiv \rho^{\bar{p}p}(s, t = 0) - \rho^{pp}(s, t = 0)$$

  are, almost all of them, well constrained.
- The discrepancy between he no-Odderon model and the experimental data in the moderate-t region (especially at $\sqrt{s} = 52.8$ GeV and $\sqrt{s} = 541$ GeV) is so big that, in their turn, the supplementary 12 free parameters (at least, most of them) are also well constrained.
- Only the $b_1^-,\ \alpha_{RP}^-(0),\ C_{RP}^+,\ \beta_O,\ \beta_R^+$ and β_R^- parameters (6 out of 35) are not well determined (more than 15% error)

The case with the Odderon

- 12 supplementary free parameters as compared with the no-Odderon case: O_k, b_k^- $(k = 1, 2, 3)$, K_-, C_O, β_O, α'_O, C_{OP} and β_{OP}
- The 23 free parameters associated with the dominant $F_+(s,t)$ amplitude and with the component of $F_-(s,t)$ responsible for describing the data for $\Delta\sigma(s)$ and $\Delta\rho(s, t = 0)$, where

$$\Delta\rho(s,t=0) \equiv \rho^{\bar{p}p}(s,t=0) - \rho^{pp}(s,t=0)$$

  are, almost all of them, well constrained.
- The discrepancy between he no-Odderon model and the experimental data in the moderate-t region (especially at $\sqrt{s} = 52.8$ GeV and $\sqrt{s} = 541$ GeV) is so big that, in their turn, the supplementary 12 free parameters (at least, most of them) are also well constrained.
- Only the b_1^-, $\alpha_{RP}^-(0)$, C_{RP}^+, β_O, β_R^+ and β_R^- parameters (6 out of 35) are not well determined (more than 15% error)

The case with the Odderon

- 12 supplementary free parameters as compared with the no-Odderon case: O_k, b_k^- $(k = 1, 2, 3)$, K_-, C_O, β_O, α'_O, C_{OP} and β_{OP}

- The 23 free parameters associated with the dominant $F_+(s,t)$ amplitude and with the component of $F_-(s,t)$ responsible for describing the data for $\Delta\sigma(s)$ and $\Delta\rho(s, t = 0)$, where

$$\Delta\rho(s, t = 0) \equiv \rho^{\bar{p}p}(s, t = 0) - \rho^{pp}(s, t = 0)$$

  are, almost all of them, well constrained.

- The discrepancy between he no-Odderon model and the experimental data in the moderate-t region (especially at $\sqrt{s} = 52.8$ GeV and $\sqrt{s} = 541$ GeV) is so big that, in their turn, the supplementary 12 free parameters (at least, most of them) are also well constrained.

- Only the b_1^-, $\alpha_{RP}^-(0)$, C_{RP}^+, β_O, β_R^+ and β_R^- parameters (6 out of 35) are not well determined (more than 15% error)

The case with the Odderon

- 12 supplementary free parameters as compared with the no-Odderon case: $O_k,\ b_k^-\ (k=1,2,3),\ K_-,\ C_O,\ \beta_O,\ \alpha'_O,\ C_{OP}$ and β_{OP}
- The 23 free parameters associated with the dominant $F_+(s,t)$ amplitude and with the component of $F_-(s,t)$ responsible for describing the data for $\Delta\sigma(s)$ and $\Delta\rho(s,t=0)$, where

$$\Delta\rho(s,t=0) \equiv \rho^{\bar{p}p}(s,t=0) - \rho^{pp}(s,t=0)$$

  are, almost all of them, well constrained.
- The discrepancy between he no-Odderon model and the experimental data in the moderate-t region (especially at $\sqrt{s}=52.8$ GeV and $\sqrt{s}=541$ GeV) is so big that, in their turn, the supplementary 12 free parameters (at least, most of them) are also well constrained.
- Only the $b_1^-,\ \alpha_{RP}^-(0),\ C_{RP}^+,\ \beta_O,\ \beta_R^+$ and β_R^- parameters (6 out of 35) are not well determined (more than 15% error)

Best-fit parameters

$$\chi^2_{dof} = 2.46\ ,\ \chi^2_{dof}\big|_{t=0} = 1.42$$

(276 experimental forward points out of a total of 832)

Parameters of $F_+^H(s,t)$

H_1 (mb)	b_1^+ (GeV^{-2})	H_2 (mb)	b_2^+ (GeV^{-2})	H_3 (mb)	b_3^+ (GeV^{-2})	K_+
0.4030 $\pm$ 0.0015	4.5691 $\pm$ 0.0677	-3.8616 $\pm$ 0.0262	7.1798 $\pm$ 0.1603	9.2079 $\pm$ 0.2091	6.0270 $\pm$ 0.0808	0.6571 $\pm$ 0.0089

Maximal Odderon parameters

O_1 (mb)	b_1^- (GeV^{-2})	O_2 (mb)	b_2^- (GeV^{-2})	O_3 (mb)	b_3^- (GeV^{-2})	K_-
-0.0690 $\pm$ 0.0043	8.9526 $\pm$ 1.6989	1.4166 $\pm$ 0.0324	3.4515 $\pm$ 0.0361	-0.3558 $\pm$ 0.0097	1.1064 $\pm$ 0.0186	0.1267 $\pm$ 0.0017

Reggeon poles and cuts parameters

	P	PP	O	OP	R_+	R_-	$(RP)_+$	$(RP)_-$
$\alpha(0)$					0.48 $\pm$ 0.01	0.34 $\pm$ 0.02	-0.56 $\pm$ 0.06	0.70 $\pm$ 0.20
C (mb)	40.43 $\pm$ 0.17	-9.20 $\pm$ 0.63	-6.07 $\pm$ 0.50	11.83 $\pm$ 1.68	38.18 $\pm$ 2.64	47.09 $\pm$ 4.84	-1930.1 $\pm$ 749.8	8592.7 $\pm$ 931.1
β (GeV)$^{-2}$	4.37 $\pm$ 0.05	1.95 $\pm$ 0.07	5.33 $\pm$ 1.60	1.73 $\pm$ 0.14	0.03 $\pm$ 4.21	33.60 $\pm$ 41.74	0.79 $\pm$ 0.14	7.33 $\pm$ 0.15
α' (GeV)$^{-2}$			0.57 $\pm$ 0.14					

Best-fit parameters

$\chi^2_{dof} = 2.46$, $\chi^2_{dof}\big|_{t=0} = 1.42$

(276 experimental forward points out of a total of 832)

Parameters of $F_+^H(s,t)$

H_1 (mb)	b_1^+ (GeV^{-2})	H_2 (mb)	b_2^+ (GeV^{-2})	H_3 (mb)	b_3^+ (GeV^{-2})	K_+
0.4030 $\pm$ 0.0015	4.5691 $\pm$ 0.0677	-3.8616 $\pm$ 0.0262	7.1798 $\pm$ 0.1603	9.2079 $\pm$ 0.2091	6.0270 $\pm$ 0.0808	0.6571 $\pm$ 0.0089

Maximal Odderon parameters

O_1 (mb)	b_1^- (GeV^{-2})	O_2 (mb)	b_2^- (GeV^{-2})	O_3 (mb)	b_3^- (GeV^{-2})	K_-
-0.0690 $\pm$ 0.0043	8.9526 $\pm$ 1.6989	1.4166 $\pm$ 0.0324	3.4515 $\pm$ 0.0361	-0.3558 $\pm$ 0.0097	1.1064 $\pm$ 0.0186	0.1267 $\pm$ 0.0017

Reggeon poles and cuts parameters

	P	PP	O	OP	R_+	R_-	$(RP)_+$	$(RP)_-$
$\alpha(0)$					0.48 $\pm$ 0.01	0.34 $\pm$ 0.02	-0.56 $\pm$ 0.06	0.70 $\pm$ 0.20
C (mb)	40.43 $\pm$ 0.17	-9.20 $\pm$ 0.63	-6.07 $\pm$ 0.50	11.83 $\pm$ 1.68	38.18 $\pm$ 2.64	47.09 $\pm$ 4.84	-1930.1 $\pm$ 749.8	8592.7 $\pm$ 931.1
β $(\mathrm{GeV})^{-2}$	4.37 $\pm$ 0.05	1.95 $\pm$ 0.07	5.33 $\pm$ 1.60	1.73 $\pm$ 0.14	0.03 $\pm$ 4.21	33.60 $\pm$ 41.74	0.79 $\pm$ 0.14	7.33 $\pm$ 0.15
α' $(\mathrm{GeV})^{-2}$			0.57 $\pm$ 0.14					

Results and predictions for $d\sigma/dt$

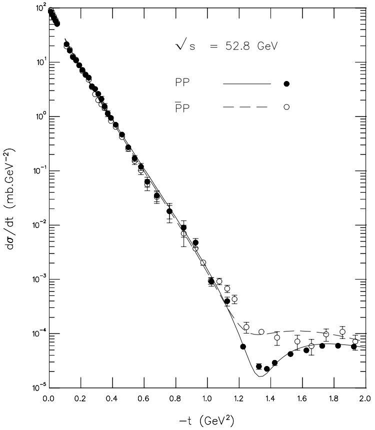

The structure (dip) region moves slowly, with increasing energy, from $|t| \approx 1.35$ GeV^2 at $\sqrt{s} = 52.8$ GeV towards $|t| \simeq 0.9$ GeV^2 at $\sqrt{s} = 500$ GeV.

Results and predictions for $d\sigma/dt$

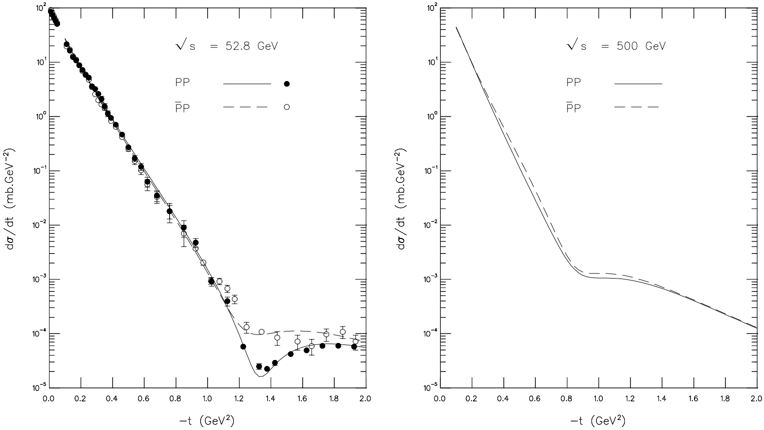

The structure (dip) region moves slowly, with increasing energy, from $|t| \approx 1.35$ GeV^2 at $\sqrt{s} = 52.8$ GeV towards $|t| \simeq 0.9$ GeV^2 at $\sqrt{s} = 500$ GeV.

Results and predictions for $d\sigma/dt$

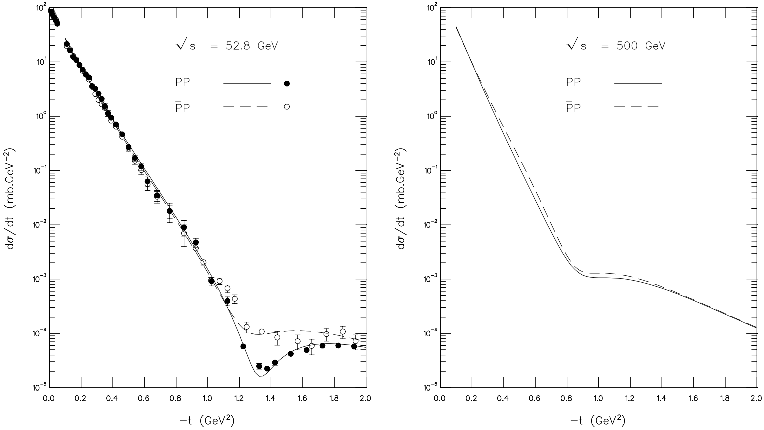

The structure (dip) region moves slowly, with increasing energy, from $|t| \approx 1.35$ GeV^2 at $\sqrt{s} = 52.8$ GeV towards $|t| \simeq 0.9$ GeV^2 at $\sqrt{s} = 500$ GeV.

Results and predictions for $d\sigma/dt$

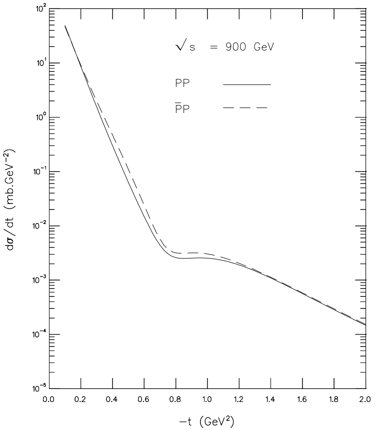

The structure (dip) region moves slowly, with increasing energy, from $|t| \approx 0.8$ GeV^2 at $\sqrt{s} = 900$ GeV towards $|t| \simeq 0.35$ GeV^2 at $\sqrt{s} = 14$ TeV.

Results and predictions for $d\sigma/dt$

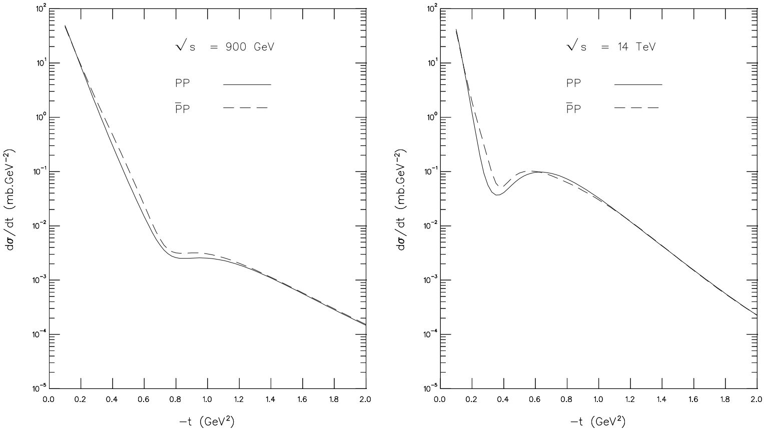

The structure (dip) region moves slowly, with increasing energy, from $|t| \approx 0.8$ GeV^2 at $\sqrt{s} = 900$ GeV towards $|t| \simeq 0.35$ GeV^2 at $\sqrt{s} = 14$ TeV.

Results and predictions for $d\sigma/dt$

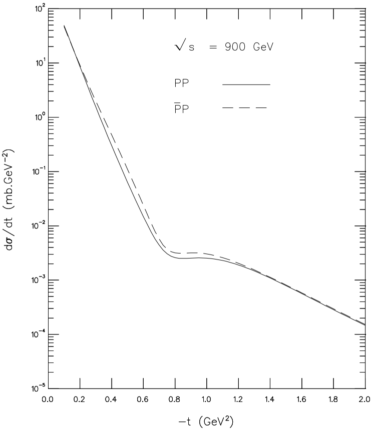

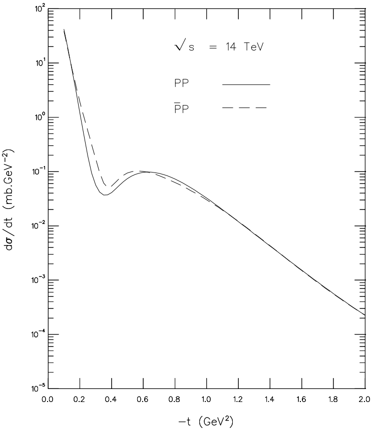

The structure (dip) region moves slowly, with increasing energy, from $|t| \approx 0.8$ GeV^2 at $\sqrt{s} = 900$ GeV towards $|t| \simeq 0.35$ GeV^2 at $\sqrt{s} = 14$ TeV.

The mechanism of the dip

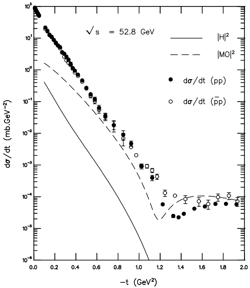

The dip is induced by the Maximal Odderon

The mechanism of the dip

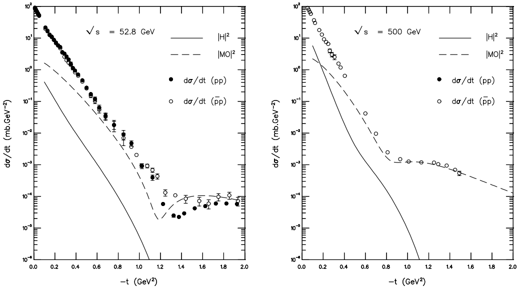

The dip is induced by the Maximal Odderon

The mechanism of the dip

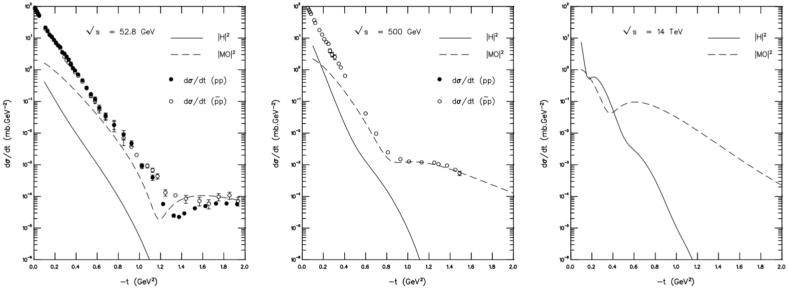

The dip is induced by the Maximal Odderon

The mechanism of the dip

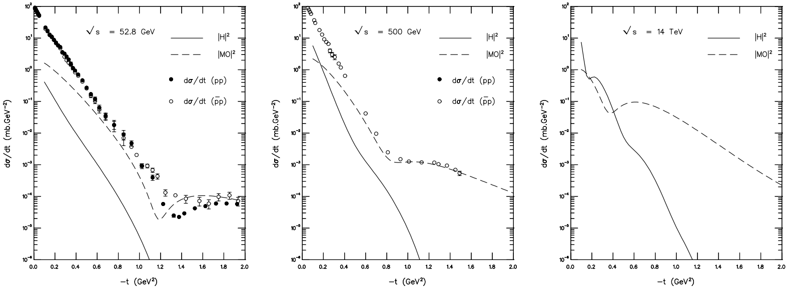

The dip is induced by the Maximal Odderon

Oscillations in the difference between the pp and $\bar{p}p$ differential cross-sections

$$\Delta \left(\frac{d\sigma}{dt} \right)(s,t) \equiv \left| \left(\frac{d\sigma}{dt} \right)^{\bar{p}p}(s,t) - \left(\frac{d\sigma}{dt} \right)^{pp}(s,t) \right|$$

Oscillations in the difference between the pp and $\bar{p}p$ differential cross-sections

$$\Delta\left(\frac{d\sigma}{dt}\right)(s,t) \equiv \left|\left(\frac{d\sigma}{dt}\right)^{\bar{p}p}(s,t) - \left(\frac{d\sigma}{dt}\right)^{pp}(s,t)\right|$$

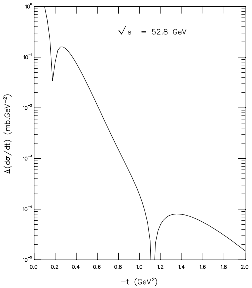

Oscillations in the difference between the pp and $\bar{p}p$ differential cross-sections

$$\Delta\left(\frac{d\sigma}{dt}\right)(s,t) \equiv \left|\left(\frac{d\sigma}{dt}\right)^{\bar{p}p}(s,t) - \left(\frac{d\sigma}{dt}\right)^{pp}(s,t)\right|$$

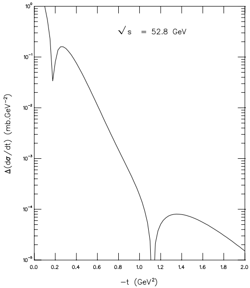

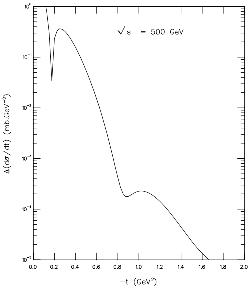

Oscillations in the difference between the pp and $\bar{p}p$ differential cross-sections

$$\Delta\left(\frac{d\sigma}{dt}\right)(s,t) \equiv \left|\left(\frac{d\sigma}{dt}\right)^{\bar{p}p}(s,t) - \left(\frac{d\sigma}{dt}\right)^{pp}(s,t)\right|$$

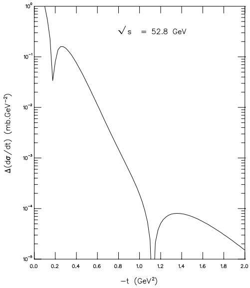

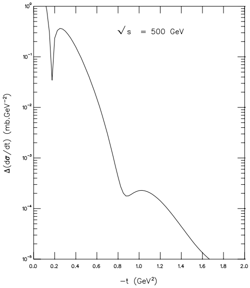

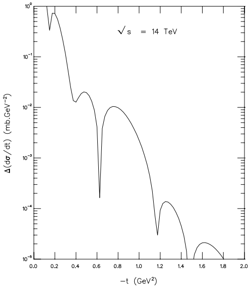

Mechanism of oscillations in $\Delta(d\sigma/dt)$

- There is an interesting phenomenon of oscillations present in $\Delta(\frac{d\sigma}{dt})$, due to the composition of the oscillations present in the Heisenberg-type amplitude $F_+^H(s,t)$ and in the Maximal Odderon amplitude $F_-^{MO}(s,t)$
- The oscillations are induced by the AKM structure at finite energies of the Heisenberg and the Maximal Odderon amplitudes
- The most interesting oscillations, from experimental point of view, are those centered around the t-value corresponding to the dip region in $d\sigma/dt$

Mechanism of oscillations in $\Delta(d\sigma/dt)$

- There is an interesting phenomenon of oscillations present in $\Delta(\frac{d\sigma}{dt})$, due to the composition of the oscillations present in the Heisenberg-type amplitude $F_+^H(s,t)$ and in the Maximal Odderon amplitude $F_-^{MO}(s,t)$
- The oscillations are induced by the AKM structure at finite energies of the Heisenberg and the Maximal Odderon amplitudes
- The most interesting oscillations, from experimental point of view, are those centered around the t-value corresponding to the dip region in $d\sigma/dt$

Mechanism of oscillations in $\Delta(d\sigma/dt)$

- There is an interesting phenomenon of oscillations present in $\Delta(\frac{d\sigma}{dt})$, due to the composition of the oscillations present in the Heisenberg-type amplitude $F_+^H(s,t)$ and in the Maximal Odderon amplitude $F_-^{MO}(s,t)$
- The oscillations are induced by the AKM structure at finite energies of the Heisenberg and the Maximal Odderon amplitudes
- The most interesting oscillations, from experimental point of view, are those centered around the t-value corresponding to the dip region in $d\sigma/dt$

How to detect oscillations in $\Delta(d\sigma/dt)$ at RHIC?

- We can not directly test the existence of these oscillations at RHIC and LHC energies, simply because we will not have both pp and $\bar{p}p$ accelerators at these energies
- However a chance to detect these oscillations at the RHIC energy $\sqrt{s} = 500$ GeV still exists, simply because the UA4/2 Collaboration already performed a high-precision $\bar{p}p$ experiment at a very close energy - 541 GeV
- By performing a very precise experiment at the RHIC energy $\sqrt{s} = 500$ GeV and by combining the corresponding pp data with the UA4/2 $\bar{p}p$ high-precision data one has a non-negligible chance to detect an oscillation centered around $|t| \simeq 0.9$ GeV^2 and therefore to detect the Odderon
- It is precisely the oscillation centered around $|t| \simeq 0.9$ GeV^2 which is the reminder of the already seen oscillation centered around $|t| \simeq 1.35$ GeV^2 at the ISR energy $\sqrt{s} = 52.8$ GeV

How to detect oscillations in $\Delta(d\sigma/dt)$ at RHIC?

- We can not directly test the existence of these oscillations at RHIC and LHC energies, simply because we will not have both *pp* and $\bar{p}p$ accelerators at these energies
- However a chance to detect these oscillations at the RHIC energy $\sqrt{s} = 500$ GeV still exists, simply because the UA4/2 Collaboration already performed a high-precision $\bar{p}p$ experiment at a very close energy - 541 GeV
- By performing a very precise experiment at the RHIC energy $\sqrt{s} = 500$ GeV and by combining the corresponding *pp* data with the UA4/2 $\bar{p}p$ high-precision data one has a non-negligible chance to detect an oscillation centered around $|t| \simeq 0.9$ GeV^2 and therefore to detect the Odderon
- It is precisely the oscillation centered around $|t| \simeq 0.9$ GeV^2 which is the reminder of the already seen oscillation centered around $|t| \simeq 1.35$ GeV^2 at the ISR energy $\sqrt{s} = 52.8$ GeV

How to detect oscillations in $\Delta(d\sigma/dt)$ at RHIC?

- We can not directly test the existence of these oscillations at RHIC and LHC energies, simply because we will not have both pp and $\bar{p}p$ accelerators at these energies
- However a chance to detect these oscillations at the RHIC energy $\sqrt{s} = 500$ GeV still exists, simply because the UA4/2 Collaboration already performed a high-precision $\bar{p}p$ experiment at a very close energy - 541 GeV
- By performing a very precise experiment at the RHIC energy $\sqrt{s} = 500$ GeV and by combining the corresponding pp data with the UA4/2 $\bar{p}p$ high-precision data one has a non-negligible chance to detect an oscillation centered around $|t| \simeq 0.9$ GeV^2 and therefore to detect the Odderon
- It is precisely the oscillation centered around $|t| \simeq 0.9$ GeV^2 which is the reminder of the already seen oscillation centered around $|t| \simeq 1.35$ GeV^2 at the ISR energy $\sqrt{s} = 52.8$ GeV

How to detect oscillations in $\Delta(d\sigma/dt)$ at RHIC?

- We can not directly test the existence of these oscillations at RHIC and LHC energies, simply because we will not have both pp and $\bar{p}p$ accelerators at these energies
- However a chance to detect these oscillations at the RHIC energy $\sqrt{s} = 500$ GeV still exists, simply because the UA4/2 Collaboration already performed a high-precision $\bar{p}p$ experiment at a very close energy - 541 GeV
- By performing a very precise experiment at the RHIC energy $\sqrt{s} = 500$ GeV and by combining the corresponding pp data with the UA4/2 $\bar{p}p$ high-precision data one has a non-negligible chance to detect an oscillation centered around $|t| \simeq 0.9$ GeV^2 and therefore to detect the Odderon
- It is precisely the oscillation centered around $|t| \simeq 0.9$ GeV^2 which is the reminder of the already seen oscillation centered around $|t| \simeq 1.35$ GeV^2 at the ISR energy $\sqrt{s} = 52.8$ GeV

How to detect the Odderon at LHC?

We predict

$$\sigma_T^{pp}(\sqrt{s} = 14 \text{ TeV}) = 123.32 \text{ mb} ,$$
$$\Delta\sigma(\sqrt{s} = 14 \text{ TeV}) = -3.92 \text{ mb} ,$$
$$\rho_{pp}(\sqrt{s} = 14 \text{ TeV},\ t = 0) = 0.103 ,$$
$$\Delta\rho(\sqrt{s} = 14 \text{ TeV},\ t = 0) = 0.094 .$$

A high-precision ρ^{pp}-measurement at LHC would be certainly a very important test of the maximal Odderon, given the fact that our prediction is sufficiently lower than what dispersion relations without Odderon contributions could predict ($\rho \simeq 0.12 - 0.14$)

We also predict

a dip centered at $|t| \simeq 0.35$ GeV^2 in $d\sigma/dt$ at $\sqrt{s} = 14$ TeV

How to detect the Odderon at LHC?

We predict

$$\sigma_T^{pp}(\sqrt{s} = 14 \text{ TeV}) = 123.32 \text{ mb} ,$$
$$\Delta\sigma(\sqrt{s} = 14 \text{ TeV}) = -3.92 \text{ mb} ,$$
$$\rho_{pp}(\sqrt{s} = 14 \text{ TeV},\ t = 0) = 0.103 ,$$
$$\Delta\rho(\sqrt{s} = 14 \text{ TeV},\ t = 0) = 0.094 .$$

A high-precision ρ^{pp}-measurement at LHC would be certainly a very important test of the maximal Odderon, given the fact that our prediction is sufficiently lower than what dispersion relations without Odderon contributions could predict ($\rho \simeq 0.12 - 0.14$)

We also predict

a dip centered at $|t| \simeq 0.35$ GeV^2 in $d\sigma/dt$ at $\sqrt{s} = 14$ TeV

Conclusions

- The most spectacular signature of the Odderon is the predicted oscillations in the difference between the differential cross-sections for proton-proton and antiproton-proton at high s and moderate t. This experiment can be done by using the STAR detector at RHIC and by combining these future data with the already present UA4/2 data.

- The Odderon could also be found by ATLAS experiment at LHC by performing a high-precision measurement of the real part of the hadron elastic scattering amplitude at small t.

- The dips at $|t| \simeq 0.9$ GeV^2 in $d\sigma/dt$ at RHIC and at $|t| \simeq 0.35$ GeV^2 at LHC would be also indications of the experimental existence of the Odderon.

Conclusions

- The most spectacular signature of the Odderon is the predicted oscillations in the difference between the differential cross-sections for proton-proton and antiproton-proton at high s and moderate t. This experiment can be done by using the STAR detector at RHIC and by combining these future data with the already present UA4/2 data.
- The Odderon could also be found by ATLAS experiment at LHC by performing a high-precision measurement of the real part of the hadron elastic scattering amplitude at small t.
- The dips at $|t| \simeq 0.9$ GeV^2 in $d\sigma/dt$ at RHIC and at $|t| \simeq 0.35$ GeV^2 at LHC would be also indications of the experimental existence of the Odderon.

Conclusions

- The most spectacular signature of the Odderon is the predicted oscillations in the difference between the differential cross-sections for proton-proton and antiproton-proton at high s and moderate t. This experiment can be done by using the STAR detector at RHIC and by combining these future data with the already present UA4/2 data.

- The Odderon could also be found by ATLAS experiment at LHC by performing a high-precision measurement of the real part of the hadron elastic scattering amplitude at small t.

- The dips at $|t| \simeq 0.9$ GeV^2 in $d\sigma/dt$ at RHIC and at $|t| \simeq 0.35$ GeV^2 at LHC would be also indications of the experimental existence of the Odderon.